

Electrochemical functionalization of nanotube films: growth of aryl chains on single-walled carbon nanotubes

Pierre R. Marcoux,^{*a} Philippe Hapiot,^b Patrick Batail^a and Jean Pinson^c

^a *Laboratoire de Chimie Inorganique, Matériaux aux Interfaces (CIMI), (CNRS FRE 2447), Université d'Angers, 2 boulevard Lavoisier, Bât. K., 49045, Angers, France*

E-mail: pierre.marcoux@epfl.ch; Fax: +44 (0)21 693 44 70; Tel: +44 (0)21 639 42 97

^b *Laboratoire de Synthèse et Electrosynthèse Organiques (SESO), (CNRS UMR 6510),*

Université de Rennes 1, Campus de Beaulieu, Bât. 10C, 35042, Rennes cedex, France

E-mail: philippe.hapiot@univ-rennes1.fr; Fax: +33 (0)2 23 23 59 39

Tel: +33 (0)2 23 23 67 32

^c *Laboratoire d'Electrochimie Moléculaire, (CNRS UMR 7591), Université Paris 7,*

2 place Jussieu, Case 7107, 75251, Paris cedex 05, France. E-mail: jean.pinson@laposte.net;

Fax: +33 (0)1 44 27 76 25; Tel: +33 (0)1 44 27 28 01

Received (in Montpellier, France) 7th August 2003, Accepted 30th October 2003

First published as an Advance Article on the web 16th January 2004

Covalent exohedral derivatizations of HiPco nanotubes, through electrochemical reduction of aryldiazonium salts, is described. Four different aryldiazonium salts have been used under the same experimental conditions: 4-bromophenyl, 4-chloromethylphenyl, 4-sulfophenyl and 4-carboxyphenyl. Derivatized samples were characterized through X-ray photoelectron spectroscopy and micro-Raman diffusion. The evolution of the spectra (area of the D-band), as a function of the number of grafted groups, led us to the conclusion that the electrochemical reduction of aryldiazonium salts into radicals gives rise to the growth of aryl chains on the sidewalls of the nanotubes.

Introduction

With novel structural, electronic and mechanical properties,^{1,2} single-walled carbon nanotubes (SWNTs) constitute an important new form of carbon that could find applications in many fields,³ depending on the possibilities to chemically modify the SWNT walls. For example, the grafting of appropriate moieties on nanotubes may provide chemical selectivity for nanotube-based SPM probes,⁴ improve solubility and ease of dispersions,^{5,6} provide specificity for SWNT-based molecular sensors,⁷ facilitate self-assembly onto surfaces,^{8,9} or provide a chemical attachment point to polymer matrices in composites.¹⁰ According to Hirsch,¹¹ the different approaches to the functionalization of SWNTs may be classified into five categories: (a) defect-group functionalization,^{12,13} (b) covalent sidewall functionalization,^{14,15} (c) noncovalent exohedral functionalization with amphiphilic molecules¹⁶ or surfactant,¹⁷ (d) noncovalent exohedral functionalization with polymers¹⁸ and (e) noncovalent endohedral functionalization with, for example, C₆₀.¹⁹ The grafting procedure considered in this article falls under the classification "covalent sidewall functionalization". It is based on the electrochemical reduction of an aryldiazonium salt. Reduction of these salts gives highly reactive aryl radicals that covalently attach to the nanotube surface. This methodology, discovered at the beginning of the nineties,²⁰ has been first applied to carbon surfaces such as glassy carbon,²¹ HOPG graphite,²² carbon fibers,²³ carbon felts²⁴ or carbon black.²⁵ It was recently applied to SWNTs, either on buckypapers²⁶ or on small individual bundles.²⁷ It constitutes a simple, flexible and promising functionalization method since it is specific (unlike methods based on strong oxidizing conditions, such as acidic treatments) and provides a one-step procedure for the grafting of a widespread variety of moieties. A large number of various aryldiazonium salts

are indeed readily available, or can be prepared from the corresponding amine.

Our approach focuses on the electrochemical functionalization of single-walled carbon nanotubes, using a buckypaper electrode. Special attention has been focused to the possibility of producing multilayer modifications through an apparent polymerization process. Three types of diazonium salts bearing different substituents on the aryl groups were used: 4-bromophenyl, 4-chloromethylphenyl, 4-sulfophenyl and 4-carboxyphenyl diazonium. The extent of sidewall derivatization can be correlated to a consistent evolution of the Raman spectra of the grafted nanotubes. In addition, comparison of the spectroscopic data coming from X-ray photoelectron spectroscopy and Raman diffusion allow us to investigate the growth of aryl chains on SWNTs.

Experimental

Reagents

As-prepared SWNTs were obtained from Carbon Nanotechnologies, Incorporated (Houston TX, <http://www.cnano-tech.com>). The method by which these nanotubes were prepared is called the HiPco process and is based on the catalytic decomposition of carbon monoxide.²⁸ They were not purified before functionalization, in order to avoid any oxidation of the tubes before grafting. The dominant impurity is the metal catalyst, which is encased in thin carbon shells (2–3 graphitic layers) and distributed throughout the sample as 2–5 nm diameter particles. We performed mass elemental analysis on as-prepared SWNTs and the following molar ratios were obtained: C/Fe = 20.8 and O/Fe = 2.1 (iron catalyst is partially oxidized). Furthermore, we observed very small amounts

of amorphous carbon. It was sometimes adsorbed on bundles, and most often on catalytic particles. Concerning the aryldiazonium salts, Fig. 1 shows the four experimented compounds. Compound **1** was obtained from Aldrich and compound **2** from Fluka. Other diazonium salts, chloromethylphenyl diazonium tetrafluoroborate (**3**) and 4-carboxyphenyl diazonium tetrafluoroborate (**4**), were prepared by standard diazotation of the corresponding amines with NaNO_2 in acidic medium.²⁴

Electrode preparation and electrochemical grafting

In order to easily handle large sheets of nanotube thin films, SWNTs were deposited on a non-adherent support. We chose as a support a filtration membrane made of Teflon (Sartorius, 1 μm ϕ) since it is porous, non-adhesive, chemically inert and electrically insulating. SWNTs are first sonicated in ethanol (spectrosol quality) for 10 min. The obtained dispersion is then immediately filtered through a 1 μm Teflon membrane, so as to deposit a thin layer of SWNTs (~ 2 μm , measured by scanning electronic microscopy) on the support. After drying, a rectangle is cut in the membrane and four holes are made at the corners. A copper wire runs through these holes, in order to form a rigid frame. Electrical contact is ensured by a silver paint point (PROVAC AG, silver print) between the copper frame and the nanotube layer. The prepared nanotube film is used as the working electrode in a three-electrode cell and immersed in an acetonitrile solution containing the aryldiazonium salt (10^{-2} M) and the supporting electrolyte (tetra-n-butylammonium hexafluorophosphate, 10^{-1} M). Care is taken not to immerse the upper part of the nanotube film supporting the silver paint point. The counter-electrode is made with a graphite crucible that serves as a container for the acetonitrile solution at room temperature. The diazonium salt is reduced by applying a potential of -1 V vs. SCE and applied for a period of 30 min. Oxygen is removed from the solution by bubbling argon during the experiment. The portion of the membrane that is not immersed in the solution is excised after reaction and the remainder is soaked in hot acetonitrile for 30 min to remove the aryldiazonium that has not reacted with the nanotube film. It is then low density sonicated at room temperature for 5 min in acetonitrile, then in chloroform, acetone and ether. During these washing, a slight fraction of the SWNTs leave the film and can be recovered through filtration. The washed functionalized nanotubes are finally dried under air at 80°C (24 h) and under primary vacuum at room temperature (48 h). We noticed that none of the functionalized samples were soluble in the solvents used for washing, nor in dimethylformamide or 1,2-dichlorobenzene.

Spectroscopic measurements

Raman data were recorded on a Jobin Yvon T64000 spectrometer (CNRS-Université de Nantes), equipped with a cooled charged coupled-device (CCD) detector. The scattering signal was collected through a microscope in a backscattering configuration. All spectra were obtained at room temperature, with

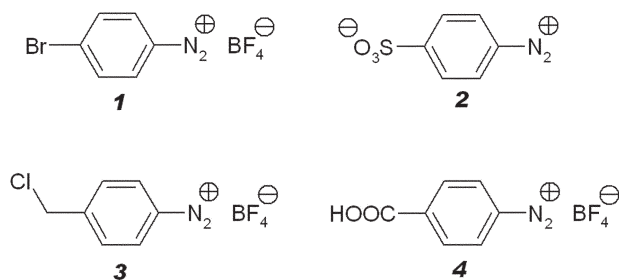


Fig. 1 Aryldiazonium salts used in this work to derivatize single-wall carbon nanotubes.

a resolution of 2 cm^{-1} . The laser power on the sample was limited to $2\text{ }\mu\text{W}$ to avoid heating of the samples.

The XPS analyses were performed with a Leybold (LHS 12) spectrometer (CNRS-Université de Nantes). The ionizing radiation ($\text{K}\alpha_{1,2}$ of Mg) was provided by a non-monochromated X-ray source, working at an acceleration tension of 12 kV and an emission current of 10 mA. Argon etching was not performed on the samples, in order to avoid any damage of the grafted groups.

Structural characterization

SWNTs were observed, before and after functionalization, with a Hitachi H9000-NAR (300 kV) transmission electron microscope (TEM). Samples were prepared by evaporating an alcoholic solution of the nanotubes onto an amorphous carbon membrane.

Results and discussion

As a first example of grafting through the reduction of an aryldiazonium salt, we chose to modify the SWNTs by 4-bromophenyl groups (**1**) since bromine atoms give a strong signal in XPS, allowing for easy detection of the bonded moieties, even at a low derivatization level. This diazonium has already been used before, for the derivatization of the same kind of SWNTs (HiPco tubes), and these experiments allow a comparison with previously published results.²⁶ 4-Chloromethylphenyl (**3**) and 4-carboxyphenyl (**4**) groups were also used with the aim of performing later chemical reaction couplings with the attached groups, either through a nucleophilic substitution of chlorine, or through an esterification reaction of the carboxylic acid. Finally, the grafting of the sulfonate compound **2** was considered as a way for providing ionic functionalized nanotubes. Due to repulsive coulombic interactions, ionic grafted SWNTs are expected to be more soluble than neutral ones.

After electrochemical modification, the SWNTs were first examined by transmission electron microscopy. Structural characterization by this technique showed that for all the considered aryldiazoniums, the tubular structure is clearly maintained after functionalization (Fig. 2). Thermogravimetric

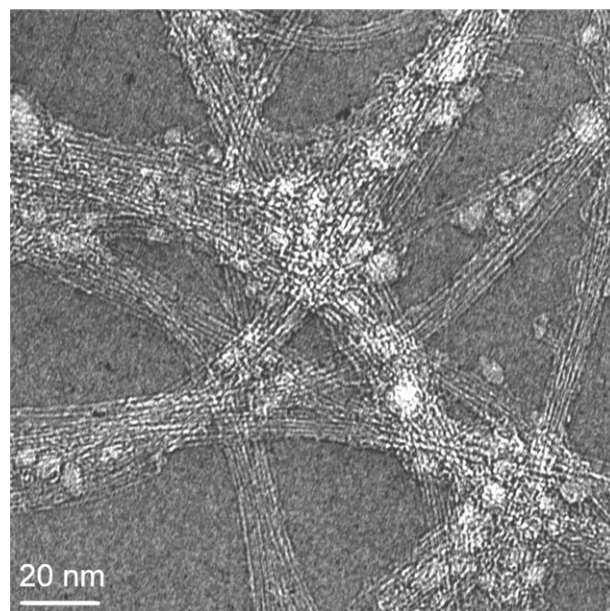


Fig. 2 High-resolution transmission electron microscopy image of a film of nanotubes, electrochemically functionalized with 4-bromophenyl diazonium.

analyses were also performed on a pristine sample and on nanotubes grafted with 4-bromophenyl groups (nanotubes were previously scratched and taken off from the Teflon membrane). The conditions for both these experiments were: $5^{\circ}\text{C min}^{-1}$, under air, from 20°C to 850°C . The thermogram of grafted nanotubes showed only one step ($510\text{--}550^{\circ}\text{C}$) of mass decrease. So it was not possible to highlight a distinct loss of mass specific to the grafted groups. Some thermal treatments were also tried under argon, at 500°C , in order to recover the pristine nanotubes and to measure the mass of grafted groups. After such a treatment we realized, through TEM observations and Raman spectroscopy, that most of the nanotubes were destroyed (loss of the breathing radial modes and very broadened tangential modes).

To more thoroughly investigate the spectroscopic characterization of the functionalized nanotubes, micro-Raman spectroscopy appears as an efficient method to detail the modifications of the structure of the sidewalls due to covalent grafting. As we have previously shown in the case of the fluorination of SWNTs,²⁹ an increasing amount of sidewall derivatization is consistent with: (i) a decrease of the relative intensities of the radial modes, without any change of the frequencies; (ii) an increase of the relative intensity of the D-band, without any frequency shift; (iii) a strong broadening of the tangential modes, with a downshifted frequency. Similar evolutions are expected after electrochemical modification due to the binding of the aryl groups on the SWNTs walls. This is indeed what we observed for the radial modes and the D-band, as illustrated in spectra a and b in Fig. 3 of a sample electrochemically grafted with 4-bromophenyl diazonium tetrafluoroborate. In contrast, the tangential modes are hardly modified after aryl grafting [Fig. 3(c)]: only a slight broadening can be seen and there is no frequency shift. The evolution we observe concerning the relative intensities of the radial modes and D-band are the same as those previously reported by Bahr *et al.*²⁶ We have tried to observe some “kinetics” of Raman D-band growth (growth of the relative area of the D-band, as a function of time during which the potential is applied). We have not managed yet to observe a clear trend because of difficulties in controlling local current densities. In our actual cell, it is indeed difficult to put the work electrode back in the same position, compared to the other two electrodes. Current research is directed towards improving our electrochemical cell.

In complement of the Raman diffusion experiments, X-ray photoelectron spectroscopy allows the determination of the stoichiometry C_nR (R = aryl group), that is the number of bonded aryl groups *versus* the number of carbons of the nanotube, by monitoring the signals specific to the elements in the grafted groups (bromine for **1**, see Fig. 1, sulfur for **2**, chlorine for **3** and oxygen for **4**). A noticeable difference between the micro-Raman experiment and XPS lies in the size of the probed region. This question becomes important when the homogeneity of a functionalized nanotube film is investigated. The probed zone with Raman diffusion is very deep, more than $10\text{ }\mu\text{m}$ (that is, more than the whole thickness of the nanotube film, about $2\text{ }\mu\text{m}$), but is not widespread in the plane of the film (about $1\text{ }\mu\text{m}$ radius). Raman spectroscopy can therefore be used as a way for checking the horizontal homogeneity, in the plane of the film. In contrast, the zone probed through XPS is widespread horizontally (several mm^2), but with very little penetration depth (around 6 nm).^{30,31} Since this sampling depth is several times larger than the diameter of a HiPco SWNT (*ca.* 0.7 nm),³² we can measure the variations of the chemical composition of SWNTs. The XPS technique can be used to test the homogeneity of the film as a function of its depth. In our case, horizontal homogeneity was investigated through Raman diffusion: all the samples, regardless of the aryl group, display the same signal intensity in all areas of the sample, indicating that all points of the surface have

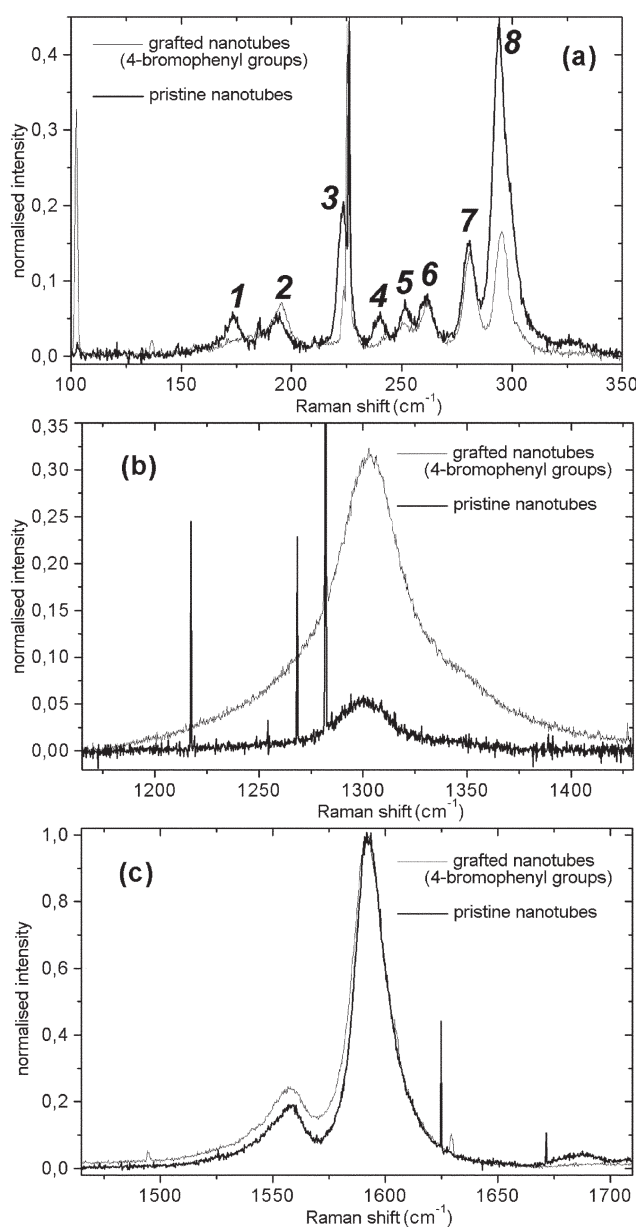


Fig. 3 Micro-Raman diffusion data collected at 676 nm . Intensities are normalized in such a way that the intensity of the strongest tangential mode is 1. Panels a, b and c plot the normalized intensities of, respectively, the radial modes, D-band and tangential modes.

equally reacted with the electrogenerated radicals. For vertical homogeneity, we can only perform XPS measurements on the upper side of the film (the one that was facing the solution during the electrochemical process) and on the lower side (the one that was facing the Teflon membrane), which led approximately to the same stoichiometry. This heterogeneity between front and back surfaces does not originate from differences of accessibility to the reagent, but from the shape of the electric current lines. The electric current at the work electrode is bigger on the side that faces the counter and reference electrodes than on the other side (the “hidden” side). Since the grafting process only occurs where electric current is, we observe a higher front surface/back surface heterogeneity for thicker electrodes. This effect also causes some difficulties in controlling local potentials. Some experiments performed with much thicker films (buckypapers being $15\text{ to }50\text{ }\mu\text{m}$ thick) yielded heterogeneously grafted zones.

Fig. 4(b) shows the XPS spectrum of a film functionalized with 4-bromophenyl groups, whereas Fig. 4(a) is the spectrum of pristine nanotubes. The two upper inserts plot the two peaks

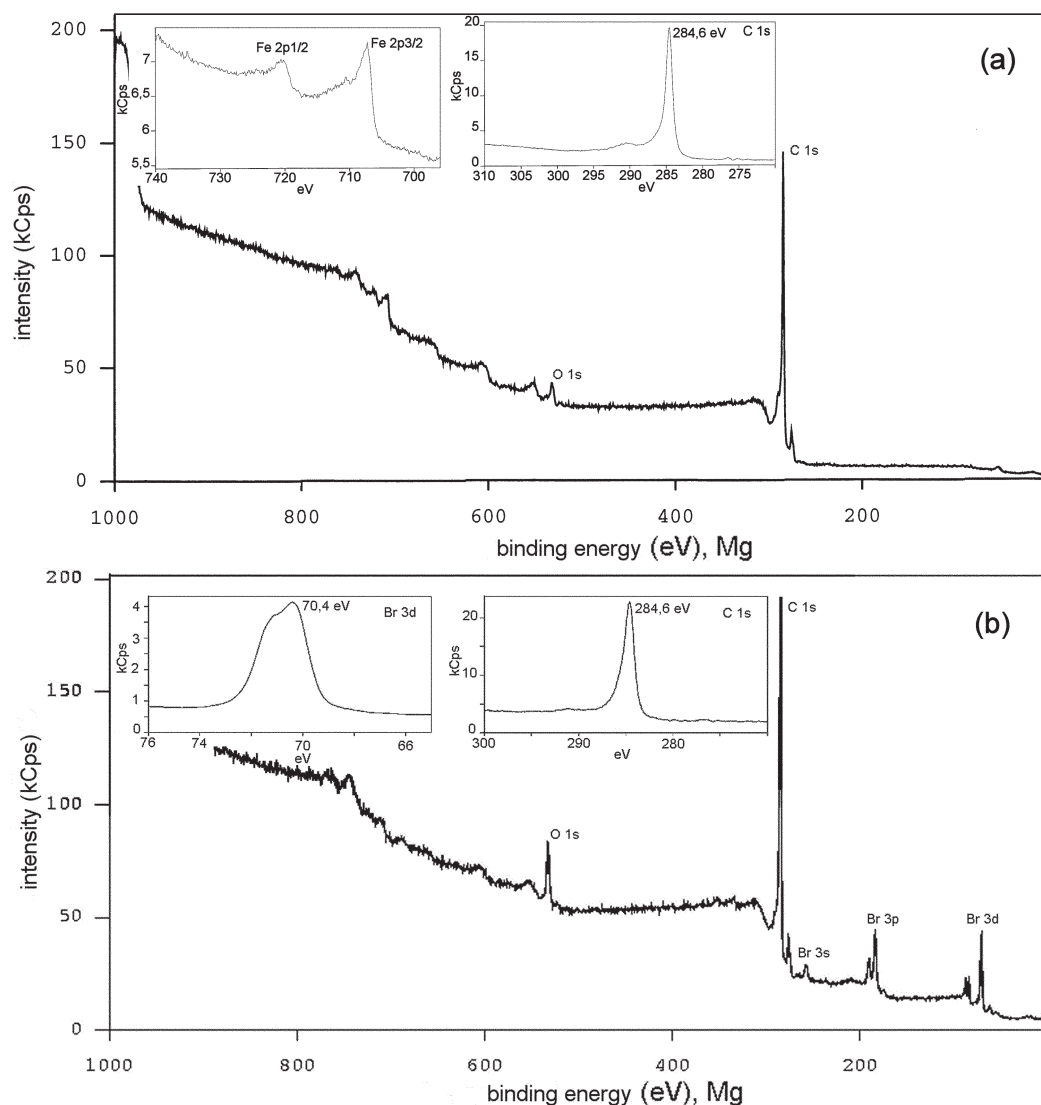


Fig. 4 (a) XPS spectrum of a film of pristine nanotubes. (b) XPS spectrum of a film of nanotubes, electrochemically functionalized with 4-bromophenyl diazonium [aryldiazonium salt: 10^{-2} M; electrolyte: $(C_4H_9)_4NPF_6$ 10^{-2} M; -1 V vs. SCE applied for 30 min]. The O 1s peak is due essentially to oxidized catalytic iron nanoparticles.

that were considered for the determination of the stoichiometry: C 1s and Br 3d. The molar percentages obtained from the integration of these peaks are C 1s = 92.0% and Br 3d = 8.0%. Among these 92 carbon atoms, about 1 stems from amorphous carbon (an impurity of HiPco tubes) and 8×6 correspond to the grafted aryls. The number n is therefore 5.4: $C_{5.4}R$. Different attempts performed with 4-bromophenyl diazonium (**1**) led to stoichiometries ranging from C_1R to $C_{13}R$ (depending on the thickness of the film). It must be emphasized that the previously reported experiments, using the same diazonium salt and the same nanotubes, yielded a $C_{25}R$ stoichiometry.²⁶ Experiments performed with **2** yielded sulfur amounts that were hardly detectable with XPS (and the Raman spectra were unchanged after functionalization). The stoichiometries were about $C_{1000}R$. This low ratio of grafted aryl groups on the nanotubes comes essentially from the low solubility of the diazonium **2** in acetonitrile. Experiments with **3** led to stoichiometries ranging from $C_{35}R$ to $C_{63}R$, and from $C_{0.4}R$ to $C_{1.6}R$ in the case of compound **4**. The values of n obtained for the diazonium compounds **1** and **4** (around 5 and even below 2) are hardly explainable if we consider just a single layer of bonded aryl moieties. Some previous works on the fluorination of SWNTs^{33,34} showed that the lower limit value of n is 2: below this value, the tubular structure is altered, contrarily to what we found from the

TEM experiments. Moreover, in our situation grafted groups will cause higher steric hindrance, the result being a lower limit for n above 2. Based on simple geometric considerations, we may expect values around 10 (in order to leave enough space between two adjacent grafted aryl groups). Such a difference cannot be explained by the presence of contaminant molecules (solvent, carbonates and hydrocarbons) adsorbed on the surface of the nanotube film: if carbon atoms coming from adsorbed impurities were considered, the number n would be even lower. Furthermore, no signals attributed to nitrogen or chlorine, elements due to the solvents acetonitrile and chloroform, could be seen [Fig. 4(b)].

In order to understand the causes of these differences, we compared the XPS and micro-Raman data originating from the same sample. Fig. 5 represents the plots of D-band integrated intensity against the stoichiometry number n derived from XPS for the different investigated compounds. The relative area of the D-band is connected with the number of covalent bonds created on the sidewalls, whereas n stems from the number of bromines bound to nanotubes. We expect the relative area of the D-band, which is proportional to the number of defects on the sidewalls, to decrease as the number n rises [Fig. 5(a)]. When n tends to infinity (pristine nanotubes), the relative area of the D-band tends to 10 (measured value for pristine HiPco tubes). The data [Figs. 5(b), 5(c) and 5(d)] do

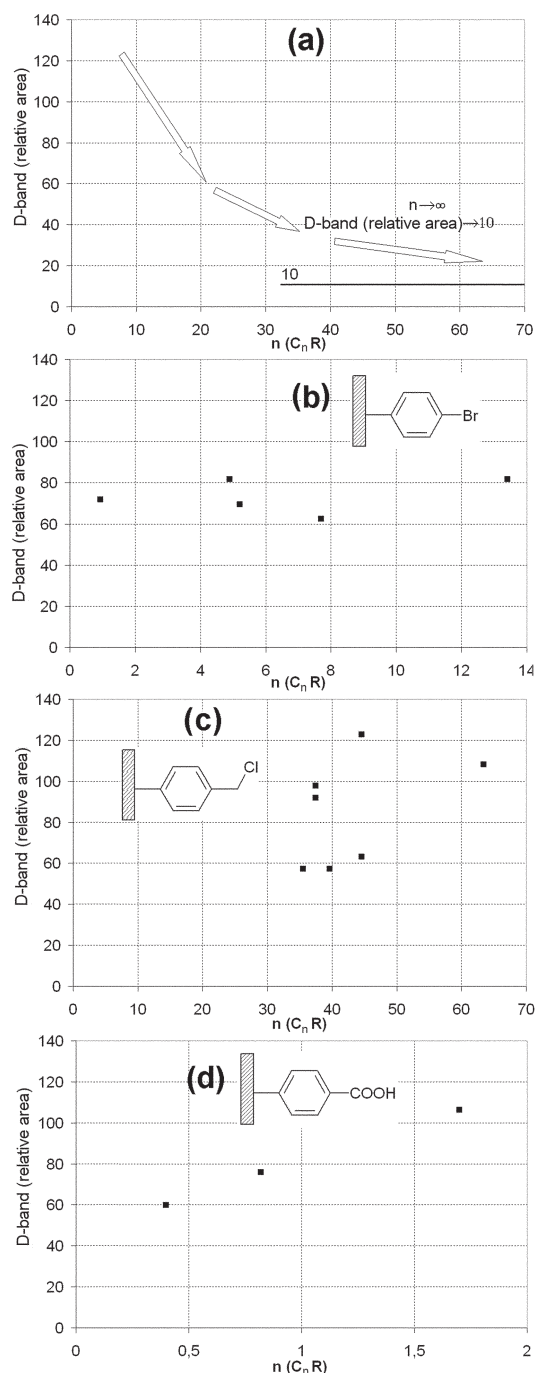


Fig. 5 Relative area of the D-band (Raman diffusion at 676 nm) plotted against the stoichiometry derived from the XPS measurements. Concerning the D-bands, the area of the strongest tangential mode, at 1592 cm⁻¹, is taken as a reference 100. Fig. 5(a) schematizes the expected downward trend. Figs. 5(b), 5(c) and 5(d) report the results for experiments performed with the diazonium salts **1**, **3** and **4**, respectively.

not follow the expected downward trend. As an example, let us focus on the results in Fig. 5(b): for different, nearly identical D-band values (areas around 70), we observe very different n values (ranging from 0.9 to 13, depending on the film of nanotubes). Fig. 5(b) shows that large and different numbers of aryl groups can be attached to the nanotube without being seen by the surface itself and thus indicate that these “extra” aryl groups are not directly linked to the walls. These results highlight a polymerization phenomenon resulting in a structure where the aryl moieties have reacted with the previously attached groups. At this point, we should remember that the

electrochemical reduction of aryldiazonium salts produces highly reactive aryl radicals near the electrode (this is the principle of the method) that are able to react not only on the nanotube surface but also on any other aromatic rings such as the already bonded aryl moieties. Such a likely reaction, between the generated aryl radicals and the moieties bound to the carbon surface, has already been reported by Kariuki and McDermott in the case of an HOPG graphite surface [Fig. 6(a)].³⁵ As far as we are concerned, this process may explain the results reported in Fig. 5, as outlined in Figs. 6(b) and 6(c), where the same number of nucleation sites on the sidewalls of SWNTs (same D-band values) would correspond to aryl chains of different lengths (different n values).

This polymerization phenomenon was considered by Bahr *et al.* in their work on the electrochemical functionalization of buckypapers,²⁶ but was rejected by the authors because of steric hindrance. This argument may eventually be justified for bulky grafting aryls, such as 4-*tert*-butylphenyl, but seems more questionable for aryl moieties such as 4-bromophenyl or 4-carboxyphenyl.³⁵ In the present experiments, our results provide new and clear evidence for the growth of aryl chains and the formation of multilayers of aryl moieties on the SWNTs for all the investigated diazonium salts.

Conclusion

The covalent bonding and growth of aryl chains on electrochemically functionalized nanotubes has been monitored by

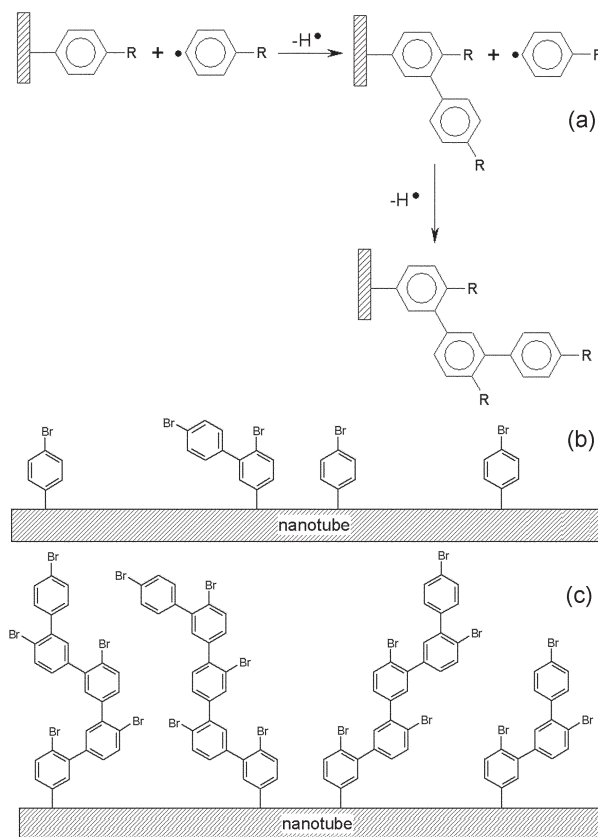


Fig. 6 (a) Grafting process of aryl radicals, in solution, onto aryl groups bound to a graphite surface.³⁵ The hydrogen atoms produced by this mechanism may react either with solvent molecules, with other aryl radicals, or with other hydrogen atoms. Illustrations (b) and (c) schematize two samples giving rise to D-bands that have the same intensity (same number of covalent bonds on the sidewalls of the nanotubes) but show different amounts of bromine in the XPS spectra. This difference can be explained through the growth of aryl chains on SWNTs.

comparison of complementary XPS and micro-Raman data. Raman diffusion gives information about the carbon backbone of SWNTs, whereas XPS informs us on the quantity of grafted moieties. Such a polymerization phenomenon (growth of aryl chains) has already been described in the literature, in the case of HOPG graphite. It is therefore not surprising to observe that a similar process occurs in the case of carbon nanotubes. Highly reactive aryl radicals react first with certain sites of the sidewalls. Then these sites of initial attack and functionalization act as nucleation sites for the subsequent growth of aryl chains. Some further studies will have to be done in order to control (or limit) the polymerisation phenomenon, by tuning experimental parameters, such as the time during which the potential is applied or the volume (steric hindrance) of the grafted moieties.

In spite of this phenomenon, electrochemical functionalization based on the electrogeneration of reactive radicals in the vicinity of the nanotube surface shows several advantages, compared to some other grafting methods, such as clean and nondestructive chemical functionalization or selective electrochemical modification of individual objects. An example has been given by Knez *et al.*³⁶ among different bundles of SWNTs deposited on a Si/SiO₂ substrate, only the bundles connected with an Au/Pd electrode were modified. The electrochemical generation of radicals also gives the hope to perform some selective chemistry on SWNTs, according to their electrical properties (metallic or semiconductive). In contrast, electrochemical functionalization has some limitations due to the fact that the reactions have to be performed on a thin film (about 2 µm) in order to get a homogeneous grafting throughout the nanotube layer. Hence, this method is not well adapted to the functionalization of large quantities of nanotubes. Furthermore, if the reaction is homogeneous at the scale of the XPS or micro-Raman probes, it may be heterogeneous on the scale of the nanotube bundles. Due to differences in accessibility for the diazonium salt, SWNTs on the outer shell of a bundle are likely to be more extensively grafted than nanotubes inside the bundle. The *in situ* generation of the diazonium species seems to be an interesting alternative to the electrochemical method,³⁷ since the grafting can be performed on dispersed nanotubes in solution. Diazonium species are generated from the aniline derivative and isoamyl nitrite. Larger amounts of SWNTs can therefore be functionalized and the problem of homogeneity is less critical.

Acknowledgements

Financial support from the CNRS and the Région Pays de Loire (Ph.D. fellowship for P.R.M.) is gratefully acknowledged. We thank V. Fernandez for assistance with the XPS measurements, C. Marhic for help with the TEM observations, J.-Y. Mévellec for participation in the Raman measurements and A. Barreau for help with the SEM observations.

References

- 1 P. M. Ajayan, *Chem. Rev.*, 1999, **99**, 1787–1799.
- 2 R. Saito, G. Dresselhaus and M. S. Dresselhaus, *Physical Properties of Carbon Nanotubes*, World Scientific, Singapore, 1998.
- 3 P. J. F. Harris, *Carbon Nanotubes and Related Structures: New Materials for the Twenty-First Century*, Cambridge University Press, Cambridge, 1999.
- 4 S. S. Wong, A. T. Woolley, E. Joselevich, C. L. Cheung and C. M. Lieber, *J. Am. Chem. Soc.*, 1998, **120**, 8557–8558.
- 5 J. Chen, A. M. Rao, S. Lyuksyutov, M. E. Itkis, M. A. Hamon, H. Hu, R. W. Cohn, P. C. Eklund, D. T. Colbert, R. E. Smalley and R. C. Haddon, *J. Phys. Chem. B*, 2001, **105**, 2525–2528.
- 6 E. T. Mickelson, I. W. Chiang, J. L. Zimmerman, P. J. Boul, J. Lozano, J. Liu, R. E. Smalley, R. H. Hauge and J. L. Margrave, *J. Phys. Chem. B*, 1999, **103**, 4318–4322.
- 7 J. Kong, M. G. Chapline and H. Dai, *Adv. Mater.*, 2001, **13**, 1384–1386.
- 8 Z. Liu, Z. Shen, T. Zhu, S. Hou and L. Ying, *Langmuir*, 2000, **16**, 3569–3573.
- 9 D. Chattopadhyay, I. Galeska and F. Papadimitrakopoulos, *J. Am. Chem. Soc.*, 2001, **123**, 9451–9452.
- 10 S. Delpeux, K. Metenier, R. Benoit, F. Vivet, L. Boufendi, S. Bonnamy and F. Béguin, *AIP Conf. Proc.*, 1999, **486**, 470–473.
- 11 A. Hirsch, *Angew. Chem., Int. Ed.*, 2002, **41**, 1853–1859.
- 12 M. A. Hamon, J. Chen, H. Hu, Y. Chen, M. E. Itkis, A. M. Rao, P. C. Eklund and R. C. Haddon, *Adv. Mater.*, 1999, **11**, 834–840.
- 13 M. A. Hamon, H. Hu, P. Bhowmik, S. Niyogi, B. Zhao, M. E. Itkis and R. C. Haddon, *Chem. Phys. Lett.*, 2001, **347**, 8–12.
- 14 P. J. Boul, E. T. Mickelson, C. B. Huffman, L. M. Ericson, I. W. Chiang, K. A. Smith, D. T. Colbert, R. H. Hauge, J. L. Margrave and R. E. Smalley, *Chem. Phys. Lett.*, 1999, **310**, 367–372.
- 15 M. Holzinger, O. Vostrowsky, A. Hirsch, F. Hennrich, M. Kappes, R. Weiss and F. Jellen, *Angew. Chem., Int. Ed.*, 2000, **40**, 4002–4005.
- 16 X. Wang, Y. Liu, W. Qiu and D. Zhu, *J. Mater. Chem.*, 2002, **12**, 1636–1639.
- 17 B. Vigolo, A. Pénicaud, C. Coulon, C. Sauder, R. Pailler, C. Journet, P. Bernier and P. Poulin, *Science*, 2000, **290**, 1331–1334.
- 18 M. J. O'Connell, P. J. Boul, L. M. Ericson, C. Huffman, Y. Wang, E. Haroz, C. Kuper, J. Tour, K. D. Ausman and R. E. Smalley, *Chem. Phys. Lett.*, 2001, **342**, 265–271.
- 19 B. W. Smith, M. Monthieux and D. E. Luzzi, *Chem. Phys. Lett.*, 1999, **315**, 31–36.
- 20 M. Delamar, R. Hitmi, J. Pinson and J.-M. Savéant, *J. Am. Chem. Soc.*, 1992, **114**, 5883–5884.
- 21 C. P. Andrieux, F. Gonzales and J. M. Savéant, *J. Am. Chem. Soc.*, 1997, **119**, 4292.
- 22 Y.-C. Liu and R. L. McCreery, *J. Am. Chem. Soc.*, 1995, **117**, 11254–11259.
- 23 M. Delamar, G. Désarmot, O. Fagebaume, R. Hitmi, J. Pinson and J.-M. Savéant, *Carbon*, 1997, **35**, 801–807.
- 24 E. Coulon, J. Pinson, J.-D. Bourzat, A. Commerçon and J. P. Pulicani, *Langmuir*, 2001, **17**, 7102–7106.
- 25 J. A. Belmont, R. M. Amici and P. Galloway, *United States Patent*, 5,851,280, December 22, 1998, (Cabot Corporation).
- 26 J. L. Bahr, J. Yang, D. V. Kosynkin, M. J. Bronikowski, R. E. Smalley and J. M. Tour, *J. Am. Chem. Soc.*, 2001, **123**, 6536–6542.
- 27 S. E. Kooi, U. Schlecht, M. Burghard and K. Kern, *Angew. Chem., Int. Ed.*, 2002, **41**, 1353–1355.
- 28 P. Nikolaev, M. J. Bronikowski, R. K. Bradley, F. Rohmund, D. T. Colbert, K. A. Smith and R. E. Smalley, *Chem. Phys. Lett.*, 1999, **313**, 91–97.
- 29 P. R. Marcoux, J. Schreiber, P. Batail, S. Lefrant, J. Renouard, G. Jacob, D. Albertini and J.-Y. Mevellec, *Phys. Chem. Chem. Phys.*, 2002, **4**, 2278–2285.
- 30 John C. Vickerman, *Surface Analysis: The Principal Techniques*, John Wiley & Sons Ltd, Chichester, 1997.
- 31 P. Cadman, G. Gossedge and J. D. Scott, *J. Elect. Spectrosc. Relat. Phenom.*, 1978, **13**, 1–6.
- 32 J. L. Bahr, E. T. Mickelson, M. J. Bronikowski, R. E. Smalley and J. M. Tour, *Chem. Commun.*, 2001, 193–194.
- 33 E. T. Mickelson, C. B. Huffman, A. G. Rinzler, R. E. Smalley, R. H. Hauge and J. L. Margrave, *Chem. Phys. Lett.*, 1998, **296**, 188–194.
- 34 K. F. Kelly, I. W. Chiang, E. T. Mickelson, R. H. Hauge, J. L. Margrave, X. Wang, G. E. Scuseria, C. Radloff and N. J. Halas, *Chem. Phys. Lett.*, 1999, **313**, 445–450.
- 35 J. K. Kariuki and M. T. McDermott, *Langmuir*, 1999, **15**, 6534–6540.
- 36 M. Knez, M. Sumser, A. M. Bittner, C. Wege, H. Jeske, S. Kooi, M. Burghard and K. Kern, *J. Electroanal. Chem.*, 2002, **522**, 70–74.
- 37 J. L. Bahr and J. M. Tour, *Chem. Mater.*, 2001, **13**, 3823–3824.